



# Remotely sensed reservoir water storage dynamics (1984-2015) and the influence of climate variability and management at global scale

Jiawei Hou<sup>1</sup>, Albert I.J.M. van Dijk<sup>1</sup>, Hylke E. Beck<sup>2</sup>, Luigi J. Renzullo<sup>1</sup>, Yoshihide Wada<sup>3</sup>

<sup>1</sup> Fenner School of Environment and Society, Australian National University, Australia

5 <sup>2</sup> Department of Civil and Environmental Engineering, Princeton University, United States of America

<sup>3</sup> International Institute for Applied Systems Analysis, Laxenburg, Austria

*Correspondence to:* Jiawei Hou (jiawei.hou@anu.edu.au)

**Abstract.** Many thousands of large dam reservoirs have been constructed worldwide during the last seventy years to increase reliable water supplies and support economic growth. Because reservoir storage measurements are generally not publicly available, so far there has been no global assessment of long-term dynamic changes in reservoir water volume. We overcame this by using optical (Landsat) and altimetry remote sensing to reconstruct monthly water storage for 6,743 reservoirs worldwide between 1984 and 2015. We relate reservoir storage to resilience and vulnerability and analyse their response to precipitation, streamflow and evaporation. We find reservoir storage has diminished substantially for 23% of reservoirs over the three decades but increased for 21%. The greatest declines were for dry basins in southeastern Australia (-29%), the USA (-10%), and eastern Brazil (-9%). The greatest gains occurred in the Nile Basin (+67%), Mediterranean basins (+31%) and southern Africa (+22%). Many of the observed reservoir changes were explained well by changes in precipitation and river inflows, emphasising the importance of multi-decadal precipitation changes for reservoir water storage, rather than changes in net evaporation or (demand-driven) dam water releases.

## 1. Introduction

20 Globally the number of large reservoirs - dams impounding more than 3 million m<sup>3</sup> (ICOLD 2020) - reached 58,713 in 2020 with a combined capacity of more than 10,000 km<sup>3</sup> (Chao et al. 2008). By 2015, reservoirs provide 30–40% of global irrigation water requirements, 17% of electricity generated, and various other services, including domestic and industrial water supply, recreation, fisheries, and flood and pollution control (Maavara et al. 2020; REN21 2016; Yoshikawa et al. 2014). With projected population increase, demand for water and electricity are also expected to increase substantially (Crist et al. 2017; Zarfl et al. 2015). More dams will likely be built to support increased irrigation for food production and to meet energy demand. For example, by 2014, there were 3,700 hydropower dams either under construction or planned worldwide. The majority of these are in developing countries, particularly in South America, Southeast Asia and Africa (Bonnema et al. 2016; Zarfl et al. 2015). However, constructing new reservoirs has become challenging due to a shortage of suitable construction sites and remaining ‘underdeveloped’ water resources, as well as increased recognition of the profound impacts



30 that impoundments have on the local population and riverine ecosystem (Grill et al. 2015; Grill et al. 2019; Lehner et al. 2011; Nilsson et al. 2005).

Adding to the challenge, evidence is emerging that existing reservoirs in some regions have experienced diminished water storage. Recent water supply failures or near-failures have occurred in the US Colorado River Basin since 2000 (Udall and  
35 Overpeck 2017), southeast Australia between 2002–2009 (Van Dijk et al. 2013), Barcelona, Spain, in 2007–2008 (March et al. 2013), Sao Paulo, Brazil, in 2014–2015 (Escobar 2015) and Cape Town, South Africa, in 2015–2017 (Sousa et al. 2018). However, it is unclear if these events are part of a global climate trend or due to local supply or demand changes. The underlying causes are also not necessarily the same in each case: reservoir storage dynamics are the net result of river inflows, net evaporation (i.e., evaporation minus direct precipitation onto the reservoir) and dam water releases to water  
40 bodies and users downstream. A change in the balance between these three terms leads to a change in the storage level. There are also interactions. The physical connection between precipitation, streamflow generation and atmospheric moisture demand creates positive feedbacks in storage volume changes: e.g., assuming the entire water supply system experiences comparable dry conditions, inflows will decrease while net evaporation and downstream demand for water releases for consumptive use will increase. To mitigate this feedback, reservoir operation rules will typically aim to reduce dam releases  
45 in response to lowering storage levels. Only a detailed analysis of the water balance of an individual reservoir can conclusively separate the contributions of these three processes to a change in water storage. However, in practice, a loss of reservoir water storage in the presence of a decrease in upstream or downstream river flows within the river system indicates that reduced precipitation conditions are the most likely cause, whereas the absence of such a precipitation and streamflow decrease, or even an increase, points towards less prudent reservoir operation, possibly in response to increased demand.  
50 Therefore, knowledge of temporal trends in reservoir storage and river flow can be combined to interpret whether trends in reservoir water storage are widespread globally, and if so, whether they are likely to be due to changing climate conditions or due to other factors. For the majority of large reservoirs, operators keep records of releases and estimated storage volume, inflows and net evaporation. Unfortunately, these data are typically not publicly available, for a variety of commercial, logistical, political and security reasons. Probably mainly because of this, so far there has been no attempt at a global  
55 assessment of long-term dynamic changes and attribution of trends in water reservoir storage.

Satellite remote sensing has been widely used to measure reservoir water height, extent and storage. Mulligan et al. (2020) developed a global geo-referenced database containing more than 38,000 georeferenced dams and their associated catchments, but without any descriptive features and measurement information. Database for Hydrological Time Series over  
60 Inland Waters (DAHITI) (Schwatke et al. 2015) and the U.S. Department of Agriculture's Foreign Agricultural Service (USDA-FAS) Global Reservoirs and Lakes Monitor (G-REALM) (Birkett et al. 2010) are the two most comprehensive dataset offering global surface water body height variations derived from satellite altimetry, such as Jason-1, Jason-2, Jason-3, TOPEX/Poseidon, and ENVISAT. Several regional and global reservoir water extent dynamics datasets were also



65 produced based on MODIS or Landsat imagery (Khandelwal et al. 2017; Ogilvie et al. 2018; Yao et al. 2019; Zhao and Gao  
2018). Reservoir volume dynamics can be estimated at either regional or global scale using existing datasets and approaches  
to derive both height and extent from remote sensing, but this approach is only suitable for a limited subset number of  
reservoirs worldwide due to wide spacing of the satellite altimetry tracks (Busker et al. 2019; Crétaux et al. 2011; Duan and  
Bastiaanssen 2013; Gao et al. 2012; Medina et al. 2010; Tong et al. 2016; Zhang et al. 2014). Messenger et al. (2016)  
70 estimated the volume of lakes and reservoirs with a surface area greater than 0.10 km<sup>2</sup> at global scale using a geo-statistical  
model based on surrounding topography information. However, these estimates were not dynamic time series, and so do not  
enhance our understanding of the influence of climate change and human activity on global reservoir storage.

In this study, we reconstructed monthly reservoir storage for 1984-2015 worldwide using satellite observations, and  
examined long-term trends of global reservoir water storage, and changes in reservoir resilience and vulnerability over the  
75 past three decades. We investigated interactions between precipitation, streamflow, evaporation, and reservoir water storage  
based on comprehensive analysis of streamflow from a multi-model ensemble and as observed at ca. 8,000 gauging stations,  
precipitation from a combination of station, satellite and forecast data, and open water evaporation estimates. Part of our  
objective was to determine the extent to which climate variability and human activity each affected global reservoir water  
volume over the past three decades.

## 80 **2. Data and methods**

### **2.1. Data**

#### **2.1.1 Surface water extent**

The Landsat-derived Global Surface Water Dataset (GSWD) (Pekel et al. 2016) provides statistics on the extent and change  
of surface water at the global scale over the past three decades at a spatial resolution of 30 m. Clouds, cloud shadows and  
85 terrain shadows cause errors or missing data for individual months, but Zhao and Gao (2018) developed an automated  
method to reduce these issues and enhance the accuracy of reservoir surface water extent estimates. They applied this  
method to produce a monthly time series of surface water extent dataset for 6,817 reservoirs worldwide, based on mapping  
of the location and high-water mark as contained in the Global Reservoir and Dam database (GRanD) (Lehner et al. 2011).  
The average coefficient of determination (*R*) between satellite-derived extent and observed elevation or volumes was  
90 improved from 0.43 to 0.84 based on the algorithm developed by Zhao and Gao (2018). The resulting data are available from  
1984 to 2015 and were used in this study.

#### **2.1.2 Surface water height**



The US Department of Agriculture’s Foreign Agricultural Service (USDA-FAS) provides near-real-time surface water height anomaly estimates every ten days for 301 lakes and reservoirs worldwide. The water surface height product (G-  
 95 REALM) was produced by a semi-automated process using data from a series of altimetry missions including Topex/Poseidon (1992-2002), Jason-1 (2002-2008), Jason-2 (2008-2016) and Jason-3 (2016-present) (Birkett et al. 2010). The root-mean-square error (RMSE) of G-REALM altimetry data is expected better than 10 cm for the largest water bodies (e.g., Lake Victoria; 67,166 km<sup>2</sup>) and better than 20 cm for smaller ones (e.g., Lake Chad; 18,751 km<sup>2</sup>) (Birkett et al. 2010). The advantage of using satellite radar altimeter to measure surface water height is that it is not affected by weather, time of  
 100 day, and vegetation or canopy cover. The G-REALM data is currently only available for lakes and reservoirs with an extent greater than 100 km<sup>2</sup> although observations for water bodies between 50–100 km<sup>2</sup> are expected in future.

**Table 1** List of the spatial data used in the analyses with source, resolution and temporal coverage of data

Name and Abbreviation	Temporal Range	Spatial Resolution	Temporal Resolution	Data Source	Notes
Global Reservoir Surface Area Dataset (GRSAD)	1984-2015	30 m	Monthly	Zhao and Gao (2018)	Surface water extent for 6,817 reservoirs worldwide
Global Reservoirs and Lakes Monitor (G-REALM)	1992-present	N/A	10-Day	US Department of Agriculture’s Foreign Agricultural Service (USDA-FAS) (Birkett et al. 2010)	Near-real-time surface water height anomaly for 301 lakes and reservoirs worldwide
earth2Observe water resources reanalysis	1980-2014	0.25°	Daily/Monthly	Schellekens et al. (2017)	Global surface runoff ensemble mean of eight state-of-the-art global models
Multi-Source Weighted-Ensemble Precipitation (MSWEP)	1979-2015	0.25°	3-Hour	Beck et al. (2017)	Global precipitation by merging gauge, satellite, and reanalysis data
The Worldwide Water (W3) model	1980-2014	0.25°	Daily/Monthly	Van Dijk et al. (2018)	Global open water evaporation (Priestley-Taylor potential evaporation)
Global Reservoir and Dam Database (GRaND)	N/A	N/A	N/A	Lehner et al. (2011)	Global 6,862 reservoir attributes
HydroBASINS	N/A	N/A	N/A	Lehner and Grill (2013)	Global watershed boundaries and sub-basin delineations

### 2.1.3 Auxiliary Data

105 Daily and monthly *in situ* river discharge observations were collated as part of previous research (Beck et al. 2020) from different national and international sources (Table S1). In total, we archived 22,710 river gauging records. Global monthly surface runoff estimates for 1984–2014 were derived from the earthH<sub>2</sub>Observe water resources reanalysis version 2 (Schellekens et al. 2017), calculated as the mean of an ensemble of eight state-of-the-art global models, including HTESSEL, SURFEX-TRIP, ORCHIDEE, WaterGAP3, JULES, W3RA, and LISFLOOD (for model details refer to



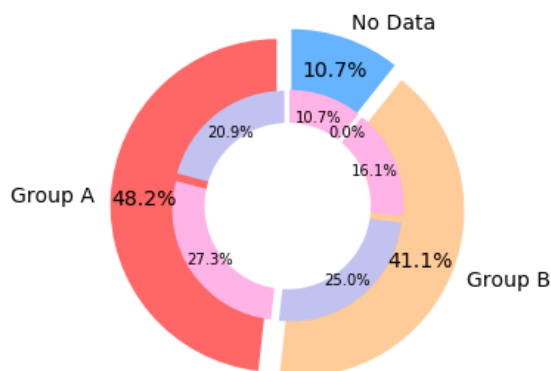
110 Schellekens et al. (2017)). Precipitation estimates were derived from a combination of station, satellite, and reanalysis data (MSWEP v1.1) (Beck et al. 2017). The representative maximum storage capacity reported in the GRanD v1.1 database (Lehner et al. 2011) was used as a reference value to calculate absolute storage changes. The HydroBASINS (Lehner and Grill 2013) dataset was used to define basin boundaries.

## 2.2 Global reservoir storage estimation

115 In total, 132 large reservoirs (Group A; Fig. 1) had records of both surface water extent and height for the overlapping period 1993–2015. We estimated the height and area at capacity as the maximum observed surface water height and extent, respectively, and calculated reservoir storage volume ( $V_o$  in GL or  $10^6$  m<sup>3</sup>) as:

$$V_o = V_c - (h_{\max} - h_o)(A_{\max} + A_o)/2 \quad (1)$$

120 where  $A_o$  (km<sup>2</sup>) is the satellite-observed water extent,  $A_{\max}$  the maximum value of  $A_o$ ,  $h_o$  (m) the satellite-observed water height,  $h_{\max}$  the maximum value of  $h_o$ , and  $V_c$  (GL) the storage volume at capacity. There were 78 reservoirs with a relationship between  $A_o$  and  $V_o$  for this overlapping period with a Pearson's  $R \geq 0.4$  (19% between 0.4-0.6, 32% between 0.6-0.8 and 49% between 0.8-1). For these reservoirs,  $V_o$  was estimated going back to 1984 using a cumulative distribution function (CDF) matching method based on  $A_o$ .



125 **Figure 1** The total storage capacity in Group A (red) and B (brown) and left unaccounted (blue) and the combined capacity of reservoirs for which the data were suitable (teal) or unsuitable (pink) for long-term analysis.

130 For 6,611 reservoirs with water extent observations only (Group B; Fig. 1), we used the HydroLAKES method (Messenger et al. 2016) to estimate storage. The mean lake or reservoir depth can be estimated using the empirical equation based on water surface area and the average slope within a 100 m buffer around the water body (Messenger et al. 2016). Four empirical equations were developed by Messenger et al. (2016) for different lake size classes (i.e., 0.1–1, 1–10, 10–100 and 100–500 km<sup>2</sup>) (Table S2). For each reservoir, water depth dynamics ( $D$  in m) from 1984-2015 were calculated using the surrounding average slope from HydroLAKES and surface water extents (Zhao and Gao 2018) based on the empirical equation



appropriate for the reservoir size. Assuming maximum observed surface water extent ( $A_{max}$ ) as the area at capacity ( $V_c$ ), a bias-corrected water depth ( $D^*$  in m) was calculated by solving  $D$  based on the ratio of water depth ( $V_c/A_{max}$  in m) at capacity and maximum observed depth ( $D_{max}$  in m):

$$D^* = \frac{D}{D_{max}} \times \frac{V_c}{A_{max}} \quad (2)$$

Storage volume ( $V_o$  in MCM) for 1984–2015 was subsequently estimated based on surface water extent ( $A_o$  in m) and bias-corrected water depth:

$$V_o = D^* A_o \quad (3)$$

Time series of *in situ* reservoir storage volume measurements are publicly available for a small subset of reservoirs. They can be used to evaluate the uncertainty in the satellite-based storage estimates. Furthermore, data records for some storages can be found in the published literature, derived from grey literature or proprietary data sources. Given the emphasis in trend analysis was on relative changes between the pre- and post-2000 periods, the evaluation of satellite-derived reservoir storage focuses on Pearson's correlation ( $R$ ) values as a measure of correspondence. In this study, we regard  $R$  values ranging from 0.4–0.7 as robust, and 0.7–1 as strong.

### 2.3 Trend analysis and attribution

We were able to estimate monthly storage dynamics for 6,743 out of the 6,862 reservoirs reported in the GRanD database (Lehner et al. 2011), accounting for 89.3% of the total 6,197 km<sup>3</sup> reported cumulative capacity (Fig. 1). There were only 132 reservoirs for which both extent and height observations were available (Group A), but this relatively small number already accounted for almost half of global combined capacity (Fig. 1). To analyse long-term changes in reservoir storage between 1984–2015, we removed all reservoirs that were destroyed, modified, planned, replaced, removed, subsumed or constructed after 1984 or for which more than five years of water extent observations needed to be interpolated because of lacking data (Zhao and Gao 2018). This left 4,589 of the initial 6,743 reservoirs available for analysis, *i.e.*, 68% of reservoirs, together accounting for 45.9% of combined global capacity (Fig. 1).

We calculated linear trends between 1984–2015 in annual reservoir storage, observed streamflow, modelled streamflow, and precipitation for each basin (HydroBASINS Level 3). Trend significance was tested using the Mann-Kendall trend test ( $p < 0.05$ ). The linear trends in modelled streamflow were validated by observed data. We also analysed the correlations between precipitation/streamflow and storage in terms of both time series and linear trend. Net evaporation was calculated for each reservoir as follows:

$$E_n = A(E_o - P) \quad (4)$$



where  $E_n$  (mm) is cumulative monthly net evaporation loss (or gain, if negative),  $A$  is reservoir surface area ( $\text{km}^2$ ) from Zhao and Gao (2018),  $E_0$  (mm) is open water evaporation (Priestley-Taylor potential evaporation from the W3 model (Van Dijk et al. 2018)), and  $P$  is precipitation (mm) from MSWEP v1.1 (Beck et al. 2017). The reservoir net evaporation summed for each basin and the ratio of the respective trends in net evaporation and storage were calculated to determine whether the former could explain the latter. Trends in storage and observed streamflow for individual reservoir and river were also analysed to provide additional information about spatial distribution of trends. Unlike the analysis at basin scale above, we do not relate the trend of each individual reservoir to a corresponding river gauge. This is because there is typically a limited number of gauging station upstream a reservoir, and as such these river flow gauging data cannot accurately represent overall reservoir inflows.

Changes in reservoir resilience, and vulnerability between 1984–1999 and 2000–2015 were analysed at the scale of river basins. The reliability, resilience and vulnerability (RRV) criteria can be used to evaluate the performance of a water supply reservoir system (Hashimoto et al. 1982; Kjeldsen and Rosbjerg 2004). The calculation requires that an unsatisfactory state can be defined in which the reservoir cannot meet all water demands, leading to a failure event. *Reliability* indicates the probability that the system is in a satisfactory state:

$$Reliability = 1 - \frac{\sum_{j=1}^M d(j)}{T} \quad (5)$$

where  $d(j)$  is the time length of the  $j^{\text{th}}$  failure event,  $T$  is the total time length, and  $M$  is the number of failure events. Unfortunately, a single threshold for failure events is not readily determined: firstly, because we did not have access to water demand and release data for each reservoir, and, secondly, because reservoirs are typically operated in response to more than a single threshold. Instead, we assumed that the reliability of each reservoir is designed to be 90%, leaving it in an unsatisfactory state for the remaining 10% of the time. This assumption made it possible to calculate resilience and vulnerability for each reservoir for the assumed 90% threshold. *Resilience* is a measure of how fast a system can return to a satisfactory state after entering a failure state:

$$Resilience = \left\{ \frac{1}{M} \sum_{j=1}^M d(j) \right\}^{-1} \quad (6)$$

*Vulnerability* describes the likely damage of failure events:

$$Vulnerability = \frac{1}{M} \sum_{j=1}^M v(j) \quad (7)$$

where  $v(j)$  is the deficit volume of the  $j^{\text{th}}$  failure events. The change in vulnerability was expressed relative to the maximum deficit volume observed.

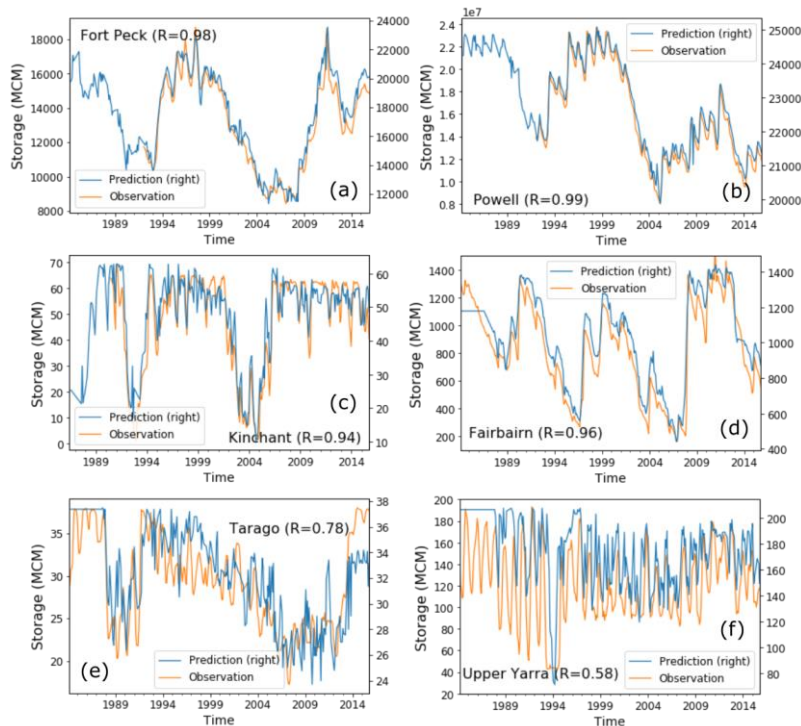




## 190 3. Results

### 3.1 Validation of global reservoir storage estimates

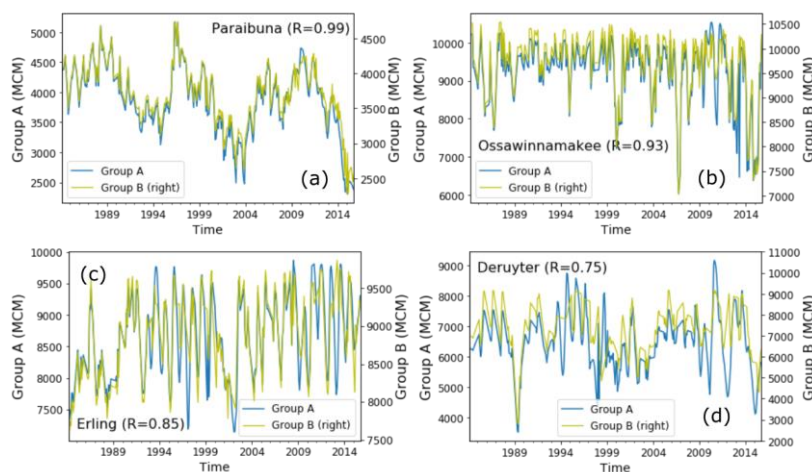
Monthly storage data with at least 20-year time series of 67 reservoirs via the US Army Corps of Engineers and Australian Bureau of Meteorology were collected. The  $R$  between published and estimated volumes was above 0.9 for 67% of the 67 reservoirs (31 reservoirs with capacity between 10-100 MCM, 25 ones between 100-1,000 MCM, 7 ones between 1,000-10,000 MCM, 4 ones with capacity above 10,000 MCM), and above 0.7 for 90% of them. Some validation examples, including robust, typical, and poor agreement are shown in Fig. 2. Annual average water levels for Lake Aswan, the largest reservoir in the world, were published as a graph (El Gammal et al. 2010); a comparison shows good agreement between the satellite-derived storage and *in situ* measurements with  $R=0.97$  (Fig. S1). Assuming the estimation method for Group A is more accurate than that for Group B, the latter can be evaluated against the former. The results show that 25 of the total 39 overlapping estimated reservoirs (3 reservoirs with capacity between 100-1,000 MCM, 27 ones between 1,000-10,000 MCM and 9 ones with capacity above 10,000 MCM) show strong agreement ( $R \geq 0.9$ ) between the two methods. Some validation examples representing good, typical, and poor agreement are shown in Fig. 3. The average Pearson correlation between our Landsat-derived water volumes and published MODIS-derived estimates (Tortini et al. 2020) from 1992 to 2015 for 100 reservoirs achieved 0.87, and the  $R$  values does not differ remarkably from different sizes of reservoirs.



205

**Figure 2** Validation of monthly reservoir storage time series reconstruction against *in situ* storage data, showing (a, b) robust, (c, d) typical and (e, f) poor results.



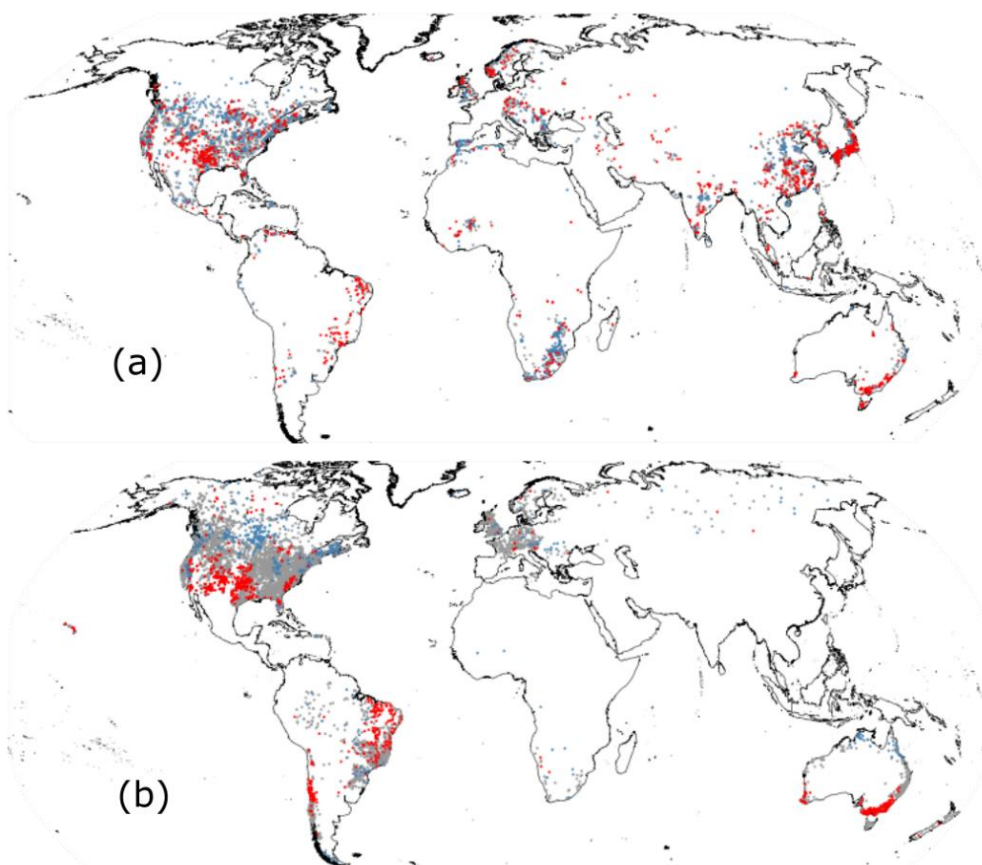


210 **Figure 3** Validation of monthly reservoir storage time series reconstruction for Group B against results obtained using the method for Group A, showing (a) robust, (b and c) typical and (d) poor agreement.

### 3.2 Changes in global reservoir storage, resilience and vulnerability

The trends ( $p < 0.05$ ) of water volume dynamics for 4,589 reservoirs and river discharge time series from around 8,000 gauging stations between 1984 and 2015 were analysis here (Fig. 4). We found no systematic global decline in reservoir water availability. Overall, there was a positive trend in combined global reservoir storage of  $+3.1 \text{ km}^3 \text{ yr}^{-1}$ , but this was almost entirely explained by positive trends for the two largest reservoirs in the world, Lake Kariba ( $+0.8 \text{ km}^3 \text{ yr}^{-1}$ ) on the Zambezi River and Lake Aswan ( $+1.9 \text{ km}^3 \text{ yr}^{-1}$ ) on the Nile River (Fig. S2). Reservoir with increasing storage trends are nearly as common as declines. 1,034 reservoirs showed decreasing trends, mainly concentrated in southwest America, eastern South America, southeast Australia and parts of Eurasia, while 948 reservoirs showed increasing trends, distributed in northern North America and southern Africa (Fig. 4a). The global reservoir storage trending pattern is similar with global river discharge tendency. In particular, a majority of rivers in southwest America, eastern South America, and southeast Australia have reduced river flows (Fig. 4b). There was no apparent relationship between primary reservoir purpose (i.e., irrigation, hydroelectric power generation, domestic water supply) and overall trend, arguably a first tentative indication that climatological influences dominate changes in release management.

215  
220



225

**Figure 4** The trends of storage (a) and observed streamflow (b) for individual reservoir and river globally ( $p < 0.05$ ; increasing: blue; no change: grey; decreasing: red).

The resilience of reservoirs in southwest America (including Mississippi Basin), central Chile, eastern South America, southeastern Australia, the coast of southeastern Africa and central Eurasia have reduced sharply between 1984 and 2015, and the vulnerability of these reservoirs have increased by more than 30% (Fig. 5). In contrast, reservoirs in western Mediterranean basins, the Nile Basin and southern Africa have stronger resilience and less vulnerability than before (Fig. 5). All these changes are attributed to changes in reservoir storage, as we found there are a robust positive relationship ( $R = 0.64$ ) between changes from the pre-2000 to the post-2000 period in storage and resilience, and a strong negative relationship ( $R = -0.79$ ) between resilience and vulnerability (Fig. 6). This means that if a reservoir has a decreasing storage, there would be a risk of falling to low capacity more often and enduring larger deficits than before. Increasing storage has the potential to create other issues, such as overtopping, dam collapse, downstream flooding caused by untimely releases during the wet season, etc. (Simonovic and Arunkumar 2016).

235

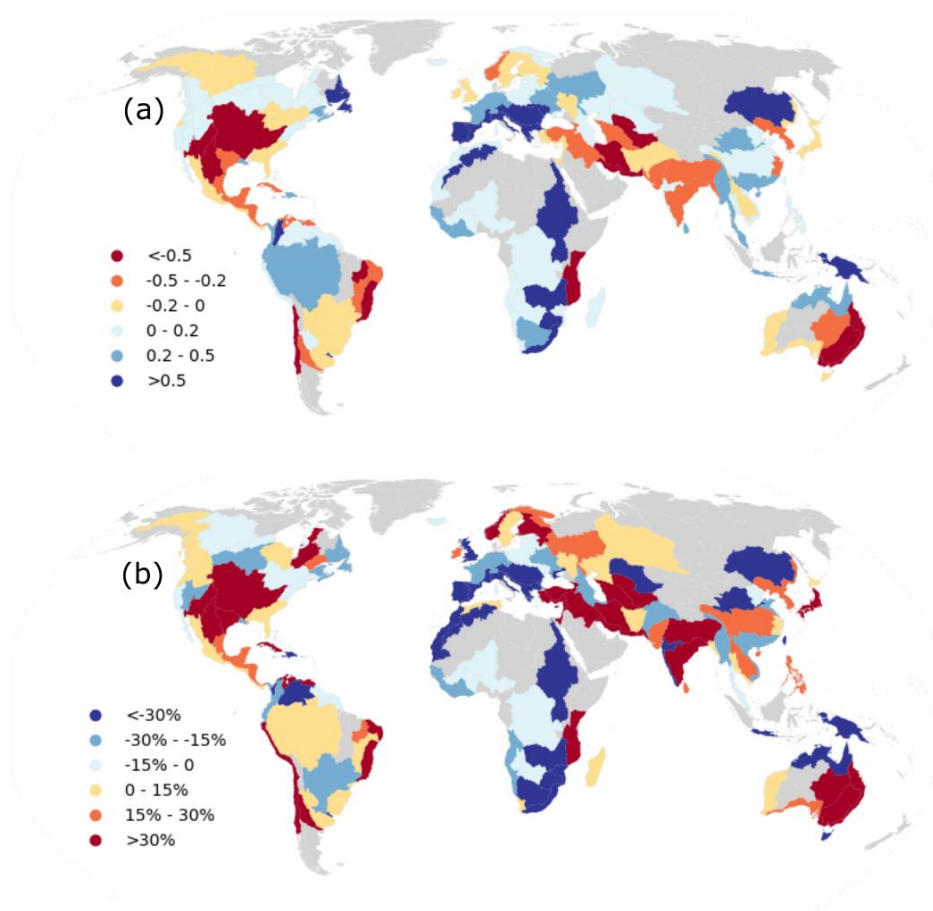


**Figure 5** The change in resilience (a), and vulnerability (b) between pre-2000 and post-2000 (grey shade: no reservoir data).

240

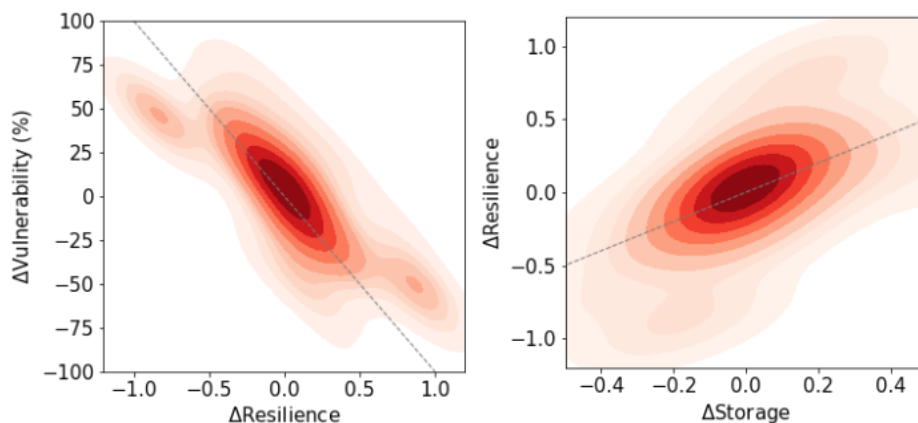
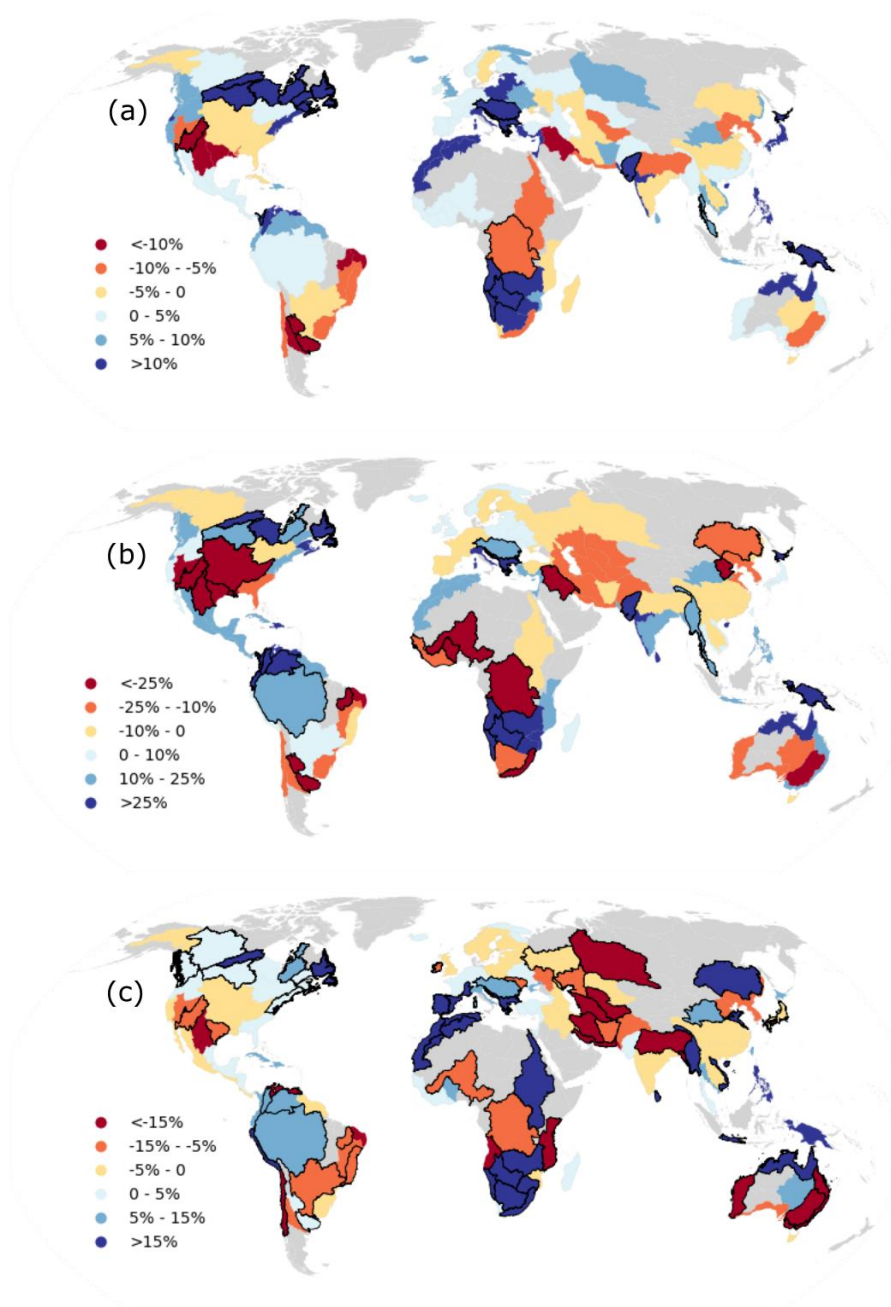


**Figure 6** The relationship (dash grey line: 1:1 line) between changes from the pre-2000 to the post-2000 period in (a) vulnerability ( $\Delta$ Vulnerability) and resilience ( $\Delta$ Resilience) and (b) mean storage ( $\Delta$ Storage) and resilience ( $\Delta$ Resilience).



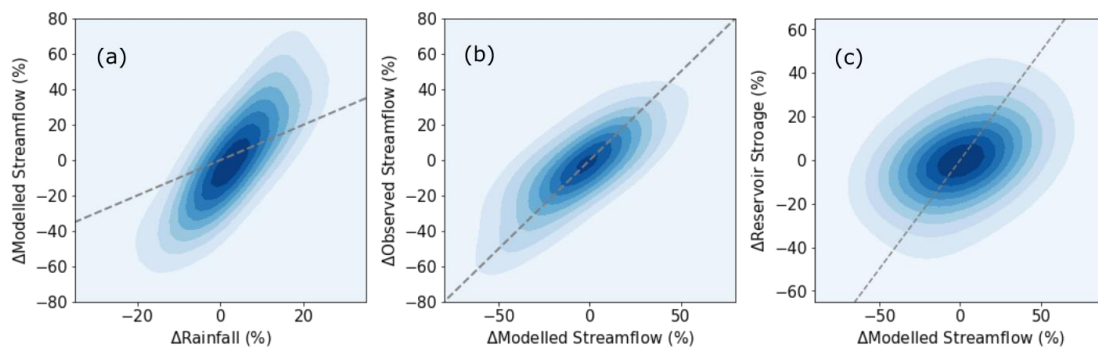
### 3.3 Influences of precipitation and river flow on global reservoir storage

245 We summed storage for individual reservoirs to calculate combined storage in 134 river basins worldwide. Basins losing or  
gaining more than 5% of their combined storage over the three decades could be found on every continent (Fig. 7c). Among  
these, 26 (19%) showed a significant decreasing and 39 (29%) a significant increasing trend in reservoir storage (Fig. 7c).  
For the majority of these 65 basins, trends were of the same sign for storage, runoff and precipitation, suggesting that  
precipitation changes are ultimately the most likely explanation for observed trends (Fig. 7a and b). Opposite trends in  
250 precipitation (or runoff) and storage were found for 12 out of 134 basins, with six decreasing and six increasing storage  
trends. Most of these could be explained by spatial variation within the respective basins (Fig. S3). The linear changes in  
modelled streamflow were validated against changes in observed streamflow, and the Pearson's correlation between them is  
0.77, which indicated modelled streamflow can reliably represent trends in river flow globally (Fig. 8b). There is a robust  
positive relationship ( $R = 0.77$ ) between linear changes from 1984-2015 in precipitation and streamflow (basin  
255 characteristics are assumed largely unchanged in the models) (Fig. 8a). A correlation above 0.6 between them can be found  
in all these 134 basin except the Niger Basin in Africa and the Parana Basin in South America (Fig. 9b). Linear changes in  
reservoir storage also have a meaningfully positive relationship ( $R = 0.38$ ,  $p < 0.01$ ,  $\rho = 0.51$ ) with streamflow (Fig. 8c),  
given the heterogeneous nature of human activities. It means a decreasing trend in streamflow (typically due to precipitation  
changes) generally leads to a decreasing trend in storage, and vice versa, but not necessarily proportionally. Figure 9a also  
260 shows that there are 59 basins that have a robust relationship between annual storage and inflow with  $R$  ranging from 0.4-  
0.8. They are mainly located in North America, southern South America, Mediterranean, southeastern Australia, and parts of  
Eurasia. These regions coincide with a large number of measured reservoirs (Fig. 4a) and a large total number of Landsat  
images over three decades (Pekel et al. 2016; Wulder et al. 2016), and vice versa. The overall relationship between reservoir  
storage and inflow might therefore be expected to be stronger if more reservoirs were measured and more useable Landsat  
265 imagery was available for those basins lacking them in our present analysis.. We also found that changes in net evaporation  
accounted for well below 10% of the overall trends in storage for each of those 65 basins, reflecting that net evaporation  
rarely explains more than a few per cent in observed storage changes (Fig. 10). In summary, we did not find evidence for  
widespread reductions in reservoir water storage due to increased releases.



270 **Figure 7** Linear trends in annual, basin-average (a) precipitation, (b) simulated streamflow and (c) reservoir storage between 1984–2015 (grey shade: no reservoir data; black outlines: trend significant at  $p < 0.05$ ).





275 **Figure 8** The relationship (dash grey line: 1: 1 line) between linear change from 1984-2015 in (a) annual precipitation ( $\Delta Rainfall$ ) and modelled streamflow ( $\Delta Modelled Streamflow$ ), (b) observed streamflow ( $\Delta Observed Streamflow$ ) and modelled streamflow ( $\Delta Modelled Streamflow$ ) and (c) reservoir storage ( $\Delta Reservoir Storage$ ) and modelled streamflow ( $\Delta Modelled Streamflow$ ).

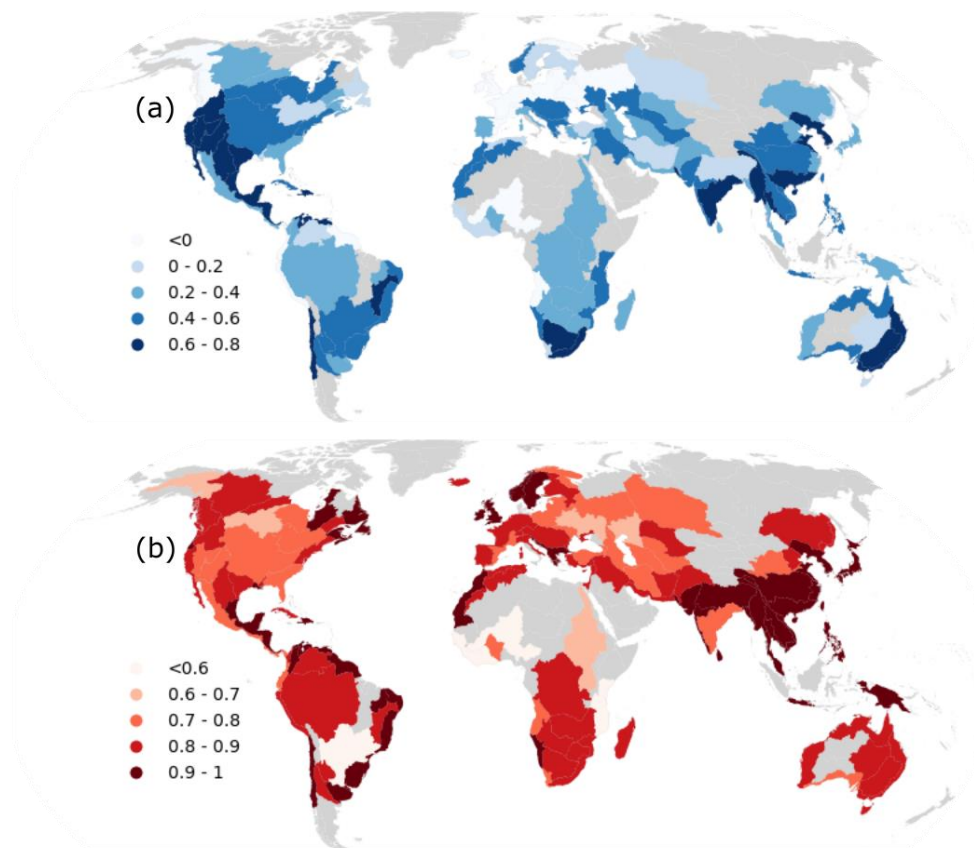
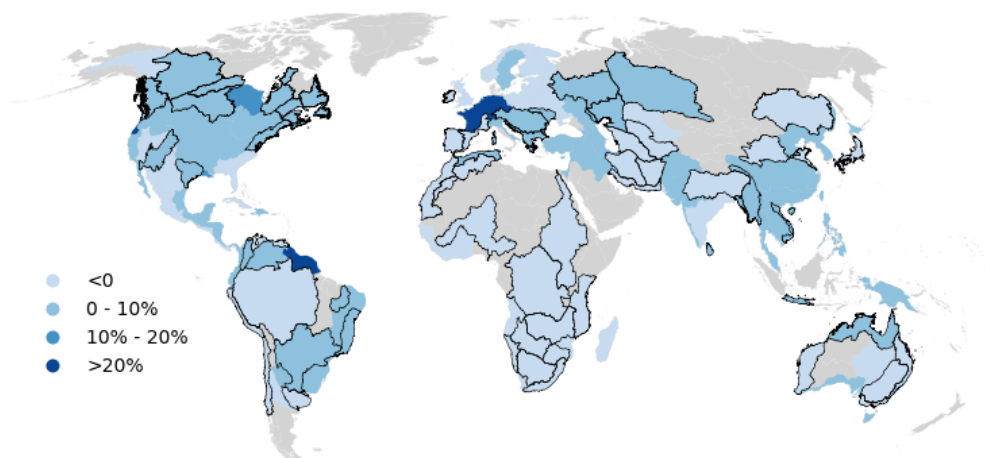


**Figure 9** The correlations of annual storage change and reservoir inflow (as approximated by basin modelled streamflow) (a), and reservoir inflow and precipitation (b) in each basin.



280

**Figure 10** The ratio of the linear trends in net evaporation and in storage in each basin.

The greatest storage gains occurred in the Nile Basin (+67%), western Mediterranean (+31%) and southern Africa (+22%), and were attributed to very high inflows during 1996-2008, 2008-2010 and 1996-2000, respectively (Fig. S4). Substantial decreases were found for arid to sub-humid basins in southeastern Australia (-29%), southwestern USA (-10%) and Brazil (-9%) (Fig. 11). Both simulated and observed river discharge data show similar trends and explain the observed storage declines (Fig. 4 and Fig. 7). During Australia's Millennium Drought (2001-2009) (Van Dijk et al. 2013), river flows in the Murray-Darling Basin fell to about half that for 1984-1999 (Fig. 11a), causing a halving of combined storage, before recovering due to high inflows during 2009-2011. In the southwestern USA, three distinct dry periods occurred (Fig. 11b). Sharp decreases in river flow after 2011 in eastern Brazil led to the lowest reservoir storage levels, with combined losses of almost 18% in 2015 (Fig. 11c). Reservoirs in these basins with reduced storage also predominantly showed reduced resilience and increased vulnerability (Fig. 5).

285  
290

#### 4 Discussion

This study reconstructed monthly reservoir water storage dynamics from 1984-2015 at global scale based on satellite-derived water extent (Zhao and Gao 2018) and altimetry measurements (Birkett et al. 2010). Where no altimetry data were available, geo-statistical models (Messenger et al. 2016) were applied to satellite-derived water extent for reservoir water volume estimation. About half (48.2%, including most large reservoirs) of total reported cumulative reservoir capacity (Lehner et al. 2011) around the world was measured by combining satellite-derived extent and height, while 41.1% was estimated based on geo-statistical models using remotely sensed surface area. There does not appear to be any systematic global decline in global reservoir water availability, but we found significantly decreasing trends in reservoir water volumes in southeastern Australia, southwestern USA and eastern Brazil, creating the risk that storages fall to low capacity more often (i.e., weakened resilience) and endure larger deficits (i.e., higher vulnerability).

300



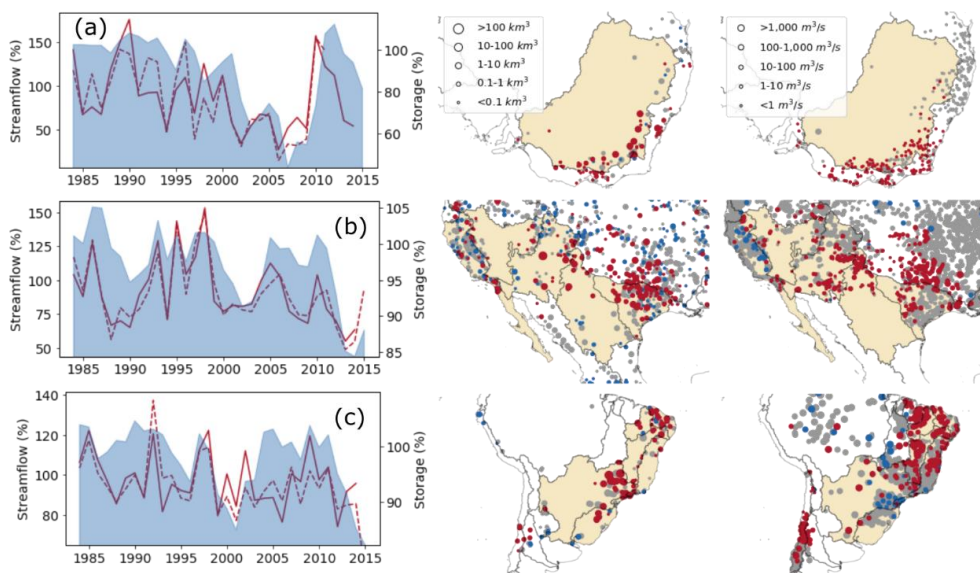


**Figure 11** Time series (left column) of annual combined storage (blue shaded) along with simulated (solid) and observed (dashed line) streamflow, indexed to the reference period 1984–1999, and trends in storage (middle column) and observed streamflow (right column) during 1984–2015 ( $p < 0.05$ ; increasing: blue; no change: grey; declining: red). Shown are (top row) southeastern Australia, (second row) southwestern USA, and (third row) Brazil.

Trends in reservoir storage and river flow showed spatial consistency at both individual and basin scales globally. There was reasonably strong temporal correlation between precipitation, streamflow and storage. Changes in net evaporation only accounted for a small fraction of reservoir volume changes. Reservoir storage dynamics ( $\Delta V$ ) are the net result of river inflows ( $Q_{in}$ ), net evaporation ( $E_n$ ) and dam (demand-related) water releases ( $Q_{out}$ ) as:

$$\Delta V = Q_{in} - E_n - Q_{out} \quad (8)$$

We found that  $\Delta V$  responds primarily to  $Q_{in}$  and that  $E_n$  does not seem to have affected  $\Delta V$ . This indicates dam (demand-related) water releases ( $Q_{out}$ ) are less likely to be the main driver of storage changes ( $\Delta V$ ).

Accurate temporal pattern estimates were the main purpose in this study because relative water storage and long-term change are more relevant information for water resources management. Our validation results show that 90% of the reservoirs evaluated show strong correlation ( $R \geq 0.7$ ) with water volume measured in situ. In terms of absolute value, water volume estimates were bias-corrected by representative maximum storage capacity from GRanD (Lehner et al. 2011) by assuming that the maximum observed surface water extent coincides with the area at full capacity. Biases remain in some reservoirs due to uncertainties in this maximum storage capacity. Representative maximum storage capacity values reported in GRanD were collected from different sources in the following order of priority: reported maximum or gross capacity, reported normal capacity and reported live or minimum capacity. These uncertainties in reported maximum capacity may have



influenced our results for individual reservoirs. This could be solved easily if more accurate reservoir storage or capacity data were available.

325 The uncertainties and limitations of reservoir storage estimates are mainly from the errors in satellite altimetry data, satellite-  
derived water extent data, and the method used to estimate bathymetry. The quality and accuracy of these altimetry  
measurements depend on the size and shape of water body, surrounding topography, surface waves, major wind events,  
heavy precipitation, tidal effects, the presence of ice and the position of the altimeter track (Birkett et al. 2010; Busker et al.  
2019). The RMSE of water level estimations of a narrow reservoir in steep terrain will be many tens of centimetres (Birkett  
330 et al. 2010; Schwatke et al. 2015). DAHITI altimetry data, with RMSE between 4–36 cm for lakes (Schwatke et al. 2015),  
should have similar accuracy as G-REALM, although its water level observations have so far received less evaluation.  
The classifier used to produce GSWD surface water data performed quite well, with less than 1% commission error and less  
than 5% of omission error (Pekel et al. 2016). But no-data classifications in GSWD data caused by cloud, ice, snow, and  
sensor-related issues could lead to large data-gaps in time series and underestimation of actual reservoir extents (Busker et  
335 al. 2019). In general, a no-data threshold is applied to monthly GSWD data for removing imagery with large percentage of  
contamination before deriving lake and reservoir water extent. It helps reduce the issue to some extent, but contaminated  
imagery would still remain in the rest of GSWD data. Zhao and Gao (2018) developed an automatic algorithm to repair  
contaminated Landsat imagery, based on which a continuous reservoir surface area datasets were produced. This has  
increased the number of effective images by 81% on average, and improved the coefficient of determination between  
340 satellite-derived extents and observed elevation or volumes from 0.735 to 0.998 for all reservoirs, from 0.598 to 0.997 for  
large reservoirs with extent above 10 km<sup>2</sup>.

There are typically two ways to estimate bathymetry based on digital elevation model (DEM) for reservoirs which have no  
satellite altimetry measurements from space. The first approach is to develop area-elevation curve based on a DEM (Avisse  
345 et al. 2017; Bonnema and Hossain 2017). The second method is to extrapolate surrounding topography from the DEM into  
the reservoir to estimate bathymetry (Messenger et al. 2016). Although the accuracy of these methods depend on errors  
inherent in DEM data, the latter one has been proven to a reliable and effective way to estimate bathymetry of global lakes  
and reservoirs. A coefficient of determination between predicted and reference depths of  $R=0.5$  ( $N=7049$ ) has been reported  
for global lakes and reservoirs (Messenger et al. 2016). Therefore, this geostatistical approach was considered appropriate to  
350 estimate reservoir volumes for reservoirs that had only satellite-derived water extent observations.

The total number of Landsat images over North America, southern South America, southern Africa, central Eurasia, and  
Australia over the past three decades is much larger than in the rest of the world, and particularly in tropical regions (Pekel et  
al. 2016; Wulder et al. 2016). Regions with sparse Landsat observations can have additional uncertainties in their long-term  
355 trend analyses, although this issue has been mitigated to some extent by the approach from Zhao and Gao (2018). In



principle, the inflow of sediments into reservoirs could contribute to decreasing storage. However, Wisser et al. (2013) showed that sedimentation caused a total decrease of global reservoir water storage of only 5% over a century (1901 to 2010), and hence we expect the effect of sedimentation on our 32-year analysis to be small.

360 Regional storage trends in the dam reservoirs found here are consistent with trends reported in a previous study for 200 lakes  
(including a few reservoirs) across North America, Europe, Asia and Africa during 1992–2019 (Kraemer et al. 2020). Both  
lakes and reservoirs are influenced by changing inflow and net evaporation in response to climate variability. Although  
human regulation has more influences on reservoirs than on natural lakes, our results suggests that overall human impacts on  
storage are less than natural influences. In line with the study carried out by Kraemer et al. (2020), we also found that the  
365 distribution of global lake and reservoir storage or level long-term trends does not fully reflect the “wet gets wetter and dry  
gets dryer” paradigm that some have predicted to occur due to anthropogenic climate change (Wang et al. 2012). Reservoirs  
in dry regions, such as southwest America, southeastern Australia and central Eurasia, have indeed seen decreasing  
combined storage, while these in wet regions, such northern North America, have increasing storage. However, at the same  
time we found increasing storage in dry southern Africa and decreasing storages in wet southeastern South America.  
370 Additionally, total terrestrial water storage (i.e., the sum of groundwater, soil water and surface water) derived from GRACE  
satellite gravimetry for the shorter period 2002-2016 showed decreases in endorheic basins in Central Eurasia and the  
southwestern USA and increases in Southern Africa consistent with our storage changes (Wang et al. 2018).

Given that reservoir storage dynamics are the net result of river inflows, net evaporation and dam (demand-related) water  
375 releases, we found a reasonable relationship between changes in river flow and reservoir storage, while changes in net  
evaporation do not seem to have affected storage trends significantly. We also infer that human activity (i.e. increased dam  
water releases) do not generally need to be invoked to explain changes in reservoir storage. However, there are no water  
demand and supply or dam operation data available globally that could serve as direct evidence, although there have been  
local studies. For example, reservoir operating rules (i.e. reservoir outflow) were inferred from a combination hydrologic  
380 modeling and satellite measurements for the Nile Basin, the Mekong Basin, northwest America, and forested region of  
Bangladesh (Bonnema and Hossain 2017; Bonnema et al. 2016; Eldardiry and Hossain 2019). It was not possible to apply  
the techniques used in these studies at global scale because of the resulting uncertainties in inferred reservoir inflows. To  
distinguish the respective influences of human activity and climate variability on reservoir dynamics, greater collaboration  
and public sharing of *in situ* data on reservoir storage, water release and downstream water use would be required. In some  
385 basins, satellite-derived upstream and downstream river discharge dynamics (Hou et al. 2020; Hou et al. 2018) and changes  
in irrigation area or evaporation (Van Dijk et al. 2018) may be able to provide additional information to better understand the  
drivers of reservoir water security. The algorithm from Zhao and Gao (2018) could in principle be used to calculate reservoir  
surface water extent time series beyond 2015, but is reliant on the availability of Landsat-derived GSWD (Pekel et al. 2016).  
Such data could also be derived from MODIS or Sentinel 2, and help understand how reservoir water storage change from



390 2015 onwards. The new NASA Surface Water and Ocean Topography (SWOT) satellite mission should also provide new  
opportunities to cover a larger number of reservoir (> 250 m<sup>2</sup>) with both surface water extent and height observations for  
storage estimations (Solander et al. 2016).

## 5. Conclusions

We reconstructed monthly storage dynamics between 1984-2015 for 6,743 reservoirs using satellite-derived water height and  
395 extent. For reservoirs with water extent data only, storage was estimated from surrounding topography. Over 90% of the  
estimated reservoir storages dynamics show robust correlations of  $\geq 0.7$  (67%  $\geq 0.9$ ) against publicly available observed  
storage volume estimates for several reservoirs in the US, Australia and Egypt. Based on the developed global dataset, we  
found that reservoir storage changed significantly in nearly half of all basins worldwide between 1984–2015, with increases  
and decreases similarly common and mostly explained by corresponding precipitation and runoff changes. Increases  
400 appeared slightly more common in cooler regions and decreases more common in drier regions. We did not find evidence  
that changes in water releases or net evaporation contributed meaningfully to global trends. Changes in reservoir water  
storage appear to be predominantly determined by periods of low inflow in response to low precipitation. Future changes in  
precipitation variability are among the most uncertain predictions by climate models (Trenberth et al. 2014). Therefore, a  
prudent approach to reservoir water management appears the only available means to avoid water supply failure for  
405 individual river systems.

**Data availability:** Global reservoir surface area dataset (GRSAD) is available from the Gao Research Group, Texas A&M  
University ([https://ceprofs.civil.tamu.edu/hgao/pages/models\\_data.html](https://ceprofs.civil.tamu.edu/hgao/pages/models_data.html)). Surface water level lake products are courtesy of  
the NASA/USDA G-REALM program and can be found at [https://ipad.fas.usda.gov/cropexplorer/global\\_reservoir/](https://ipad.fas.usda.gov/cropexplorer/global_reservoir/). GRanD  
410 (<http://globaldamwatch.org/grand/>), HydroBASINS (<https://hydrosheds.org/page/hydrobasins>) and HydroLAKES  
(<https://www.hydrosheds.org/page/hydrolakes>) products were developed by Global HydroLAB, McGill University. *In situ*  
reservoir storage data were collected from Australian Bureau of Meteorology (<http://www.bom.gov.au/waterdata/>) and the  
US Army Corps of Engineers (<http://www.nwd-mr.usace.army.mil/rcc/projdata/projdata.html>).

415 **Author contribution:** JH and AIJMVD conceived the idea. AIJMVD, HEB, LJR and YW guided the study. JH carried out  
the analysis and wrote the manuscript with contributions from all the co-authors.

**Competing interests.** The authors declare that they have no conflict of interest.

420 **Acknowledgments:** This study was supported by the ANU-CSC (the Australian National University and the China  
Scholarship Council) Scholarship. Calculations were performed on the high-performance computing system, Raijin, from the



National Computational Infrastructure (NCI), which is supported by the Australian Government. We also thank Prof. Bernhard Lehner of McGill University for his feedback on an earlier version of this paper.

## References:

- 425 Avisse, N., Tilmant, A., Müller, M.F., & Zhang, H. (2017). Monitoring small reservoirs' storage with satellite remote sensing in inaccessible areas. *Hydrology & Earth System Sciences*, 21
- Beck, H.E., van Dijk, A.I.J.M., Levizzani, V., Schellekens, J., Miralles, D.G., Martens, B., & de Roo, A. (2017). MSWEP: 3-hourly 0.25 global gridded precipitation (1979-2015) by merging gauge, satellite, and reanalysis data. *Hydrology and Earth System Sciences*, 21, 589
- 430 Beck, H.E., Wood, E.F., McVicar, T.R., Zambrano-Bigiarini, M., Alvarez-Garreton, C., Baez-Villanueva, O.M., Sheffield, J., & Karger, D.N. (2020). Bias correction of global high-resolution precipitation climatologies using streamflow observations from 9372 catchments. *Journal of Climate*, 33, 1299-1315
- Birkett, C.M., Reynolds, C., Beckley, B., & Doorn, B. (2010). From Research to Operations: The USDA Global Reservoir and Lake Monitor, chapter 2 in 'Coastal Altimetry', Springer Publications, eds. S. Vignudelli, A.G. Kostianoy, P. Cipollini and J. Benveniste.
- 435 Bonnema, M., & Hossain, F. (2017). Inferring reservoir operating patterns across the Mekong Basin using only space observations. *Water Resources Research*, 53, 3791-3810
- Bonnema, M., Sikder, S., Miao, Y., Chen, X., Hossain, F., Ara Pervin, I., Mahbubur Rahman, S., & Lee, H. (2016). Understanding satellite - based monthly - to - seasonal reservoir outflow estimation as a function of hydrologic controls.
- 440 *Water Resources Research*, 52, 4095-4115
- Busker, T., de Roo, A., Gelati, E., Schwatke, C., Adamovic, M., Bisselink, B., Pekel, J.-F., & Cottam, A. (2019). A global lake and reservoir volume analysis using a surface water dataset and satellite altimetry. *Hydrology and Earth System Sciences*, 23, 669-690
- Chao, B.F., Wu, Y., & Li, Y. (2008). Impact of artificial reservoir water impoundment on global sea level. *Science*, 320, 212-214
- 445 Crétaux, J.-F., Jelinski, W., Calmant, S., Kouraev, A., Vuglinski, V., Bergé-Nguyen, M., Gennero, M.-C., Nino, F., Del Rio, R.A., & Cazenave, A. (2011). SOLS: A lake database to monitor in the Near Real Time water level and storage variations from remote sensing data. *Advances in space research*, 47, 1497-1507
- Crist, E., Mora, C., & Engelman, R. (2017). The interaction of human population, food production, and biodiversity protection. *Science*, 356, 260-264
- 450 Duan, Z., & Bastiaanssen, W.G.M. (2013). Estimating water volume variations in lakes and reservoirs from four operational satellite altimetry databases and satellite imagery data. *Remote Sensing of Environment*, 134, 403-416
- El Gammal, E.A., Salem, S.M., & El Gammal, A.E.A. (2010). Change detection studies on the world's biggest artificial lake (Lake Nasser, Egypt). *The Egyptian Journal of Remote Sensing and Space Science*, 13, 89-99



- 455 Eldardiry, H., & Hossain, F. (2019). Understanding reservoir operating rules in the transboundary Nile river basin using macroscale hydrologic modeling with satellite measurements. *Journal of Hydrometeorology*, *20*, 2253-2269
- Escobar, H. (2015). Drought triggers alarms in Brazil's biggest metropolis. *Science*, *347*, 812-812
- Gao, H., Birkett, C., & Lettenmaier, D.P. (2012). Global monitoring of large reservoir storage from satellite remote sensing. *Water Resources Research*, *48*
- 460 Grill, G., Lehner, B., Lumsdon, A.E., MacDonald, G.K., Zarfl, C., & Liermann, C.R. (2015). An index-based framework for assessing patterns and trends in river fragmentation and flow regulation by global dams at multiple scales. *Environmental Research Letters*, *10*, 015001
- Grill, G., Lehner, B., Thieme, M., Geenen, B., Tickner, D., Antonelli, F., Babu, S., Borrelli, P., Cheng, L., & Crochetiere, H. (2019). Mapping the world's free-flowing rivers. *Nature*, *569*, 215
- 465 Hashimoto, T., Stedinger, J.R., & Loucks, D.P. (1982). Reliability, resiliency, and vulnerability criteria for water resource system performance evaluation. *Water Resources Research*, *18*, 14-20
- Hou, J., van Dijk, A.I., & Beck, H.E. (2020). Global satellite-based river gauging and the influence of river morphology on its application. *Remote Sensing of Environment*, *239*, 111629
- Hou, J., Van Dijk, A.I.J.M., Renzullo, L.J., & Vertessy, R.A. (2018). Using modelled discharge to develop satellite-based river gauging: a case study for the Amazon Basin. *Hydrology and Earth System Science*, *22*, 6435-6448
- 470 ICOLD (2020). The International Commission on Large Dams. [https://www.icold-cigb.org/GB/world\\_register/general\\_synthesis.asp](https://www.icold-cigb.org/GB/world_register/general_synthesis.asp)
- Khandelwal, A., Karpatne, A., Marlier, M.E., Kim, J., Lettenmaier, D.P., & Kumar, V. (2017). An approach for global monitoring of surface water extent variations in reservoirs using MODIS data. *Remote Sensing of Environment*, *202*, 113-128
- 475 Kjeldsen, T.R., & Rosbjerg, D. (2004). Choice of reliability, resilience and vulnerability estimators for risk assessments of water resources systems. *Hydrological Sciences Journal*, *49*
- Kraemer, B.M., Seimon, A., Adrian, R., & McIntyre, P.B. (2020). Worldwide lake level trends and responses to background climate variation. *Hydrology and Earth System Sciences*, *24*, 2593-2608
- 480 Lehner, B., & Grill, G. (2013). Global river hydrography and network routing: baseline data and new approaches to study the world's large river systems. *Hydrological Processes*, *27*, 2171-2186
- Lehner, B., Liermann, C.R., Revenga, C., Vörösmarty, C., Fekete, B., Crouzet, P., Döll, P., Endejan, M., Frenken, K., & Magome, J. (2011). High-resolution mapping of the world's reservoirs and dams for sustainable river-flow management. *Frontiers in Ecology and the Environment*, *9*, 494-502
- 485 Maavara, T., Chen, Q., Van Meter, K., Brown, L.E., Zhang, J., Ni, J., & Zarfl, C. (2020). River dam impacts on biogeochemical cycling. *Nature Reviews Earth & Environment*
- March, H., Domenech, L., & Saurí, D. (2013). Water conservation campaigns and citizen perceptions: the drought of 2007–2008 in the Metropolitan Area of Barcelona. *Natural Hazards*, *65*, 1951-1966





- 490 Medina, C., Gomez-Enri, J., Alonso, J.J., & Villares, P. (2010). Water volume variations in Lake Izabal (Guatemala) from in  
situ measurements and ENVISAT Radar Altimeter (RA-2) and Advanced Synthetic Aperture Radar (ASAR) data products.  
*Journal of Hydrology*, 382, 34-48
- 495 Messenger, M.L., Lehner, B., Grill, G., Nedeva, I., & Schmitt, O. (2016). Estimating the volume and age of water stored in  
global lakes using a geo-statistical approach. *Nature communications*, 7, 13603
- Mulligan, M., van Soesbergen, A., & Sáenz, L. (2020). GOODD, a global dataset of more than 38,000 georeferenced dams.  
*Scientific data*, 7, 1-8
- 500 Nilsson, C., Reidy, C.A., Dynesius, M., & Revenga, C. (2005). Fragmentation and flow regulation of the world's large river  
systems. *Science*, 308, 405-408
- Ogilvie, A., Belaud, G., Massuel, S., Mulligan, M., Le Goulven, P., & Calvez, R. (2018). Surface water monitoring in small  
water bodies: potential and limits of multi-sensor Landsat time series. *Hydrology and Earth System Sciences*, 22, 4349
- 500 Pekel, J.-F., Cottam, A., Gorelick, N., & Belward, A.S. (2016). High-resolution mapping of global surface water and its  
long-term changes. *Nature*, 540, 418-422
- REN21 (2016). Renewables 2016. Global Status Report. REN21. <https://www.ren21.net/gsr-2016/>
- Schellekens, J., Dutra, E., la Torre, A.M.-d., Balsamo, G., van Dijk, A., Weiland, F.S., Minvielle, M., Calvet, J.-C.,  
Decharme, B., Eisner, S., Fink, G., Flörke, M., Peßenteiner, S., van Beek, R., Polcher, J., Beck, H., Orth, R., Calton, B.,  
505 Burke, S., Dorigo, W., & Weedon, G.P. (2017). A global water resources ensemble of hydrological models: The  
earth2Observe Tier-1 dataset. *Earth System Science Data*, 9, 389-413
- Schwatke, C., Dettmering, D., Bosch, W., & Seitz, F. (2015). DAHITI—an innovative approach for estimating water level  
time series over inland waters using multi-mission satellite altimetry. *Hydrology and Earth System Sciences* 19 (10): 4345-  
4364
- 510 Simonovic, S.P., & Arunkumar, R. (2016). Comparison of static and dynamic resilience for a multipurpose reservoir  
operation. *Water Resources Research*, 52, 8630-8649
- Solander, K.C., Reager, J.T., & Famiglietti, J.S. (2016). How well will the Surface Water and Ocean Topography (SWOT)  
mission observe global reservoirs? *Water Resources Research*, 52, 2123-2140
- 515 Sousa, P.M., Blamey, R.C., Reason, C.J., Ramos, A.M., & Trigo, R.M. (2018). The ‘Day Zero’ Cape Town drought and the  
poleward migration of moisture corridors. *Environmental Research Letters*, 13, 124025
- Tong, X., Pan, H., Xie, H., Xu, X., Li, F., Chen, L., Luo, X., Liu, S., Chen, P., & Jin, Y. (2016). Estimating water volume  
variations in Lake Victoria over the past 22 years using multi-mission altimetry and remotely sensed images. *Remote Sensing  
of Environment*, 187, 400-413
- 520 Tortini, R., Noujdina, N., Yeo, S., Ricko, M., Birkett, C.M., Khandelwal, A., Kumar, V., Marlier, M.E., & Lettenmaier, D.P.  
(2020). Satellite-based remote sensing data set of global surface water storage change from 1992 to 2018. *Earth System  
Science Data*, 12, 1141-1151





- Trenberth, K.E., Dai, A., Van Der Schrier, G., Jones, P.D., Barichivich, J., Briffa, K.R., & Sheffield, J. (2014). Global warming and changes in drought. *Nature Climate Change*, 4, 17-22
- Udall, B., & Overpeck, J. (2017). The twenty - first century Colorado River hot drought and implications for the future. *Water Resources Research*, 53, 2404-2418
- 525 Van Dijk, A.I., Beck, H.E., Crosbie, R.S., de Jeu, R.A., Liu, Y.Y., Podger, G.M., Timbal, B., & Viney, N.R. (2013). The Millennium Drought in southeast Australia (2001–2009): Natural and human causes and implications for water resources, ecosystems, economy, and society. *Water Resources Research*, 49, 1040-1057
- Van Dijk, A.I.J.M., Schellekens, J., Yebra, M., Beck, H.E., Renzullo, L.J., Weerts, A., & Donchyts, G. (2018). Global 5 km  
530 resolution estimates of secondary evaporation including irrigation through satellite data assimilation. *Hydrology and Earth System Science*, 22, 4959-4980
- Wang, B., Liu, J., Kim, H.-J., Webster, P.J., & Yim, S.-Y. (2012). Recent change of the global monsoon precipitation (1979–2008). *Climate Dynamics*, 39, 1123-1135
- Wang, J., Song, C., Reager, J.T., Yao, F., Famiglietti, J.S., Sheng, Y., MacDonald, G.M., Brun, F., Schmied, H.M., &  
535 Marston, R.A. (2018). Recent global decline in endorheic basin water storages. *Nature Geoscience*, 11, 926-932
- Wisser, D., Frohling, S., Hagen, S., & Bierkens, M.F. (2013). Beyond peak reservoir storage? A global estimate of declining water storage capacity in large reservoirs. *Water Resources Research*, 49, 5732-5739
- Wulder, M.A., White, J.C., Loveland, T.R., Woodcock, C.E., Belward, A.S., Cohen, W.B., Fosnight, E.A., Shaw, J., Masek, J.G., & Roy, D.P. (2016). The global Landsat archive: Status, consolidation, and direction. *Remote Sensing of Environment*,  
540 185, 271-283
- Yao, F., Wang, J., Wang, C., & Crétaux, J.-F. (2019). Constructing long-term high-frequency time series of global lake and reservoir areas using Landsat imagery. *Remote Sensing of Environment*, 232, 111210
- Yoshikawa, S., Cho, J., Yamada, H.G., Hanasaki, N., & Kanae, S. (2014). An assessment of global net irrigation water requirements from various water supply sources to sustain irrigation: rivers and reservoirs (1960–2050). *Hydrology and  
545 Earth System Sciences*, 18, 4289-4310
- Zarfl, C., Lumsdon, A.E., Berlekamp, J., Tydecks, L., & Tockner, K. (2015). A global boom in hydropower dam construction. *Aquatic Sciences*, 77, 161-170
- Zhang, S., Gao, H., & Naz, B.S. (2014). Monitoring reservoir storage in South Asia from multisatellite remote sensing. *Water Resources Research*, 50, 8927-8943
- 550 Zhao, G., & Gao, H. (2018). Automatic correction of contaminated images for assessment of reservoir surface area dynamics. *Geophysical Research Letters*, 45, 6092-6099